

1  
2  
3  
4  
5  
6  
7  
8  
9  
10  
11  
12  
13  
14  
15

*Journal of Geophysical Research: Solid Earth*

Supporting Information for

**Changes in Crack Shape and Saturation in Laboratory-Induced Seismicity by Water Infiltration in the Transversely Isotropic Case with Vertical Cracks**

Koji Masuda

Geological Survey of Japan, National Institute of Advanced Industrial Science and Technology

**Contents of this file**

Text S1  
Figures S1 to S2

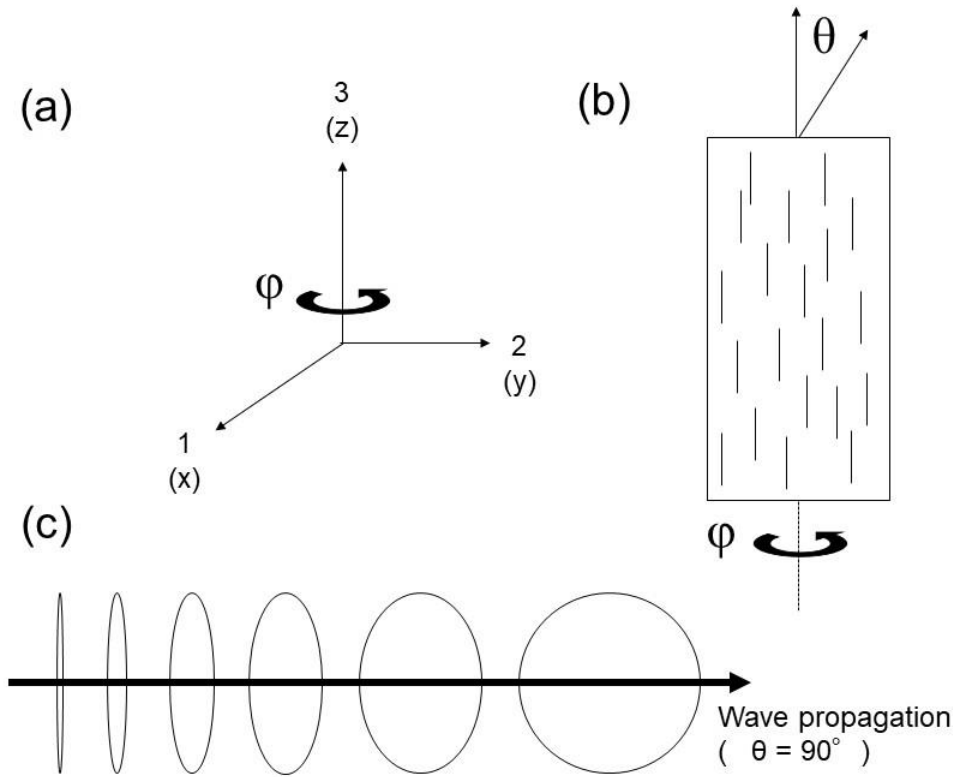
16 **Elastic constants of rock material for the case of transversely isotropic symmetry**  
 17 **along the x-3 axis (z-axis) with randomly distributed vertical cracks**

18  
 19 Here we describe the method of calculation of elastic constants for the case in which  
 20 plane normals of cracks are randomly distributed in directions perpendicular to the x-3  
 21 axis (z-axis). We also show that the ratio of the elastic constant of rock material that  
 22 includes cracks to that of the matrix or the square of velocity ratio is expressed as  $(V/V_0)^2$   
 23  $= 1 - p_i \varepsilon$ , where  $V$  and  $V_0$  are the elastic-wave velocities with and without cracks,  
 24 respectively, and  $\varepsilon$  is the crack density parameter defined by  
 25

$$\varepsilon = \frac{3 \phi}{4 \pi \alpha},$$

26  
 27 where  $\phi$  is the porosity and  $\alpha = c/a$  is the aspect ratio of the crack ( $a = b \gg c$ ). In  
 28 addition, we derive the coefficients  $p_i$ .

29  
 30 The focus of this study is on a transversely isotropic medium with the x-3 axis (z-axis) as  
 31 the axis of symmetry and with a vertical crack distribution in which the plane normals of  
 32 the cracks are randomly distributed in horizontal directions (directions parallel to the x-  
 33 1,2 plane, x-y plane). The right-handed rectangular coordinate system is used in this  
 34 study (Figure S1a).  
 35

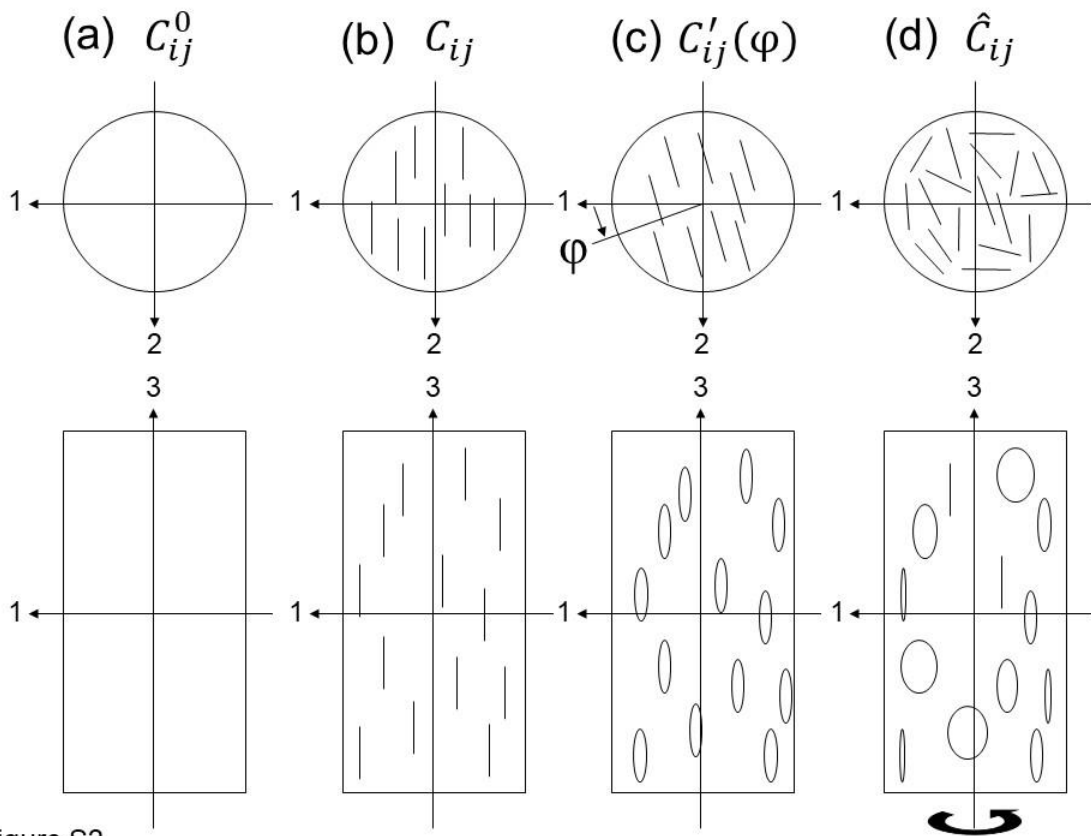


36 Figure S1

37 **Figure S1.** The basic assumptions in this study: (a) the coordinate system, (b) vertical  
 38 cross section of transversely isotropic rock with vertical cracks, and (c) side view of the  
 39 direction of wave propagation and crack distribution.

40  
 41  
 42  
 43  
 44  
 45  
 46  
 47  
 48  
 49

First, based on the method of Hudson (1981), we calculated  $C_{ij}$  for a material that  
 includes vertical cracks that are plane normal along the x-1 axis (x-axis) (Figure S1b).  
 Next, we took the rotational average of  $C_{ij}$  around the x-3 axis (z-axis), resulting in  $\hat{C}_{ij}$ ,  
 which were shown to be transversely isotropic with the x-3 axis (z-axis) by using a  
 method similar to that of Nishizawa and Masuda (1991).



50

Figure S2

51 **Figure S2.** Procedure for calculating the elastic constants in the transversely isotropic  
 52 rock with vertical cracks: (a)  $C_{ij}^0$  elastic constants of the rock matrix; (b)  $C_{ij}$  elastic  
 53 constants for the rock material with vertical cracks for which the plane-normal direction  
 54 is along the x-1 axis (x-axis); (c)  $C'_{ij}(\varphi)$  elastic constants for rock material with vertical  
 55 cracks for which the angle between the plane-normal direction and the x-1 axis (x-axis) is  
 56  $\varphi$ ; and (d)  $\hat{C}_{ij}$  elastic constants for rock material with transversely isotropic symmetry  
 57 along the x-3 axis (z-axis) with vertical cracks with random values of  $\varphi$ .

58

59 **1.  $C_{ij}^0$  elastic constants of the isotropic rock matrix (Figure S2a)**

60

61 In this study, we use abbreviated 2-index Voigt notation to express elastic constants such  
 62 as  $C_{ij}$  instead of 4-index notation for the fourth-rank tensor  $c_{ijkl}$ . We assume that the  
 63 matrix of rock without cracks or inclusions is isotropic with two independent constants:  
 64

$$C_{ij}^0 = \begin{pmatrix} C_{11}^0 & C_{12}^0 & C_{12}^0 & 0 & 0 & 0 \\ C_{12}^0 & C_{11}^0 & C_{12}^0 & 0 & 0 & 0 \\ C_{12}^0 & C_{12}^0 & C_{11}^0 & 0 & 0 & 0 \\ 0 & 0 & 0 & C_{44}^0 & 0 & 0 \\ 0 & 0 & 0 & 0 & C_{44}^0 & 0 \\ 0 & 0 & 0 & 0 & 0 & C_{44}^0 \end{pmatrix} = \begin{pmatrix} \lambda + 2\mu & \lambda & \lambda & 0 & 0 & 0 \\ \lambda & \lambda + 2\mu & \lambda & 0 & 0 & 0 \\ \lambda & \lambda & \lambda + 2\mu & 0 & 0 & 0 \\ 0 & 0 & 0 & \mu & 0 & 0 \\ 0 & 0 & 0 & 0 & \mu & 0 \\ 0 & 0 & 0 & 0 & 0 & \mu \end{pmatrix}$$

65

$$C_{12}^0 = C_{11}^0 - 2C_{44}^0$$

66

67 The relationships between the elements  $C_{ij}^0$  and Lamé's parameters  $\lambda$  and  $\mu$  of isotropic  
 68 linear elasticity are

69

$$C_{11}^0 = \lambda + 2\mu, \quad C_{12}^0 = \lambda, \quad C_{44}^0 = \mu.$$

70

71

72 **2.  $C_{ij}$  elastic constants for rock material with cracks that are plane normal along  
 73 the x-1 axis (x-axis) (Figure S2b)**

74

75 Hudson (1981) modeled fractured rock as an elastic solid with thin, penny-shaped  
 76 ellipsoidal cracks or inclusions. The effective moduli  $C_{ij}$  are given as  
 77

78

$$C_{ij} = C_{ij}^0 + C_{ij}^1,$$

79

80 where  $C_{ij}^0$  are the isotropic background moduli and  $C_{ij}^1$  are the first-order corrections. For  
 81 the case in which the vertical cracks have crack normals along the x-1 axis (x-axis), the  
 82 axis of symmetry of the material lies along the x-1 axis (x-axis), which has hexagonal  
 83 symmetry with five independent constants as  
 84

85

$$C_{ij}^1 = \begin{pmatrix} C_{11}^1 & C_{12}^1 & C_{12}^1 & 0 & 0 & 0 \\ C_{12}^1 & C_{22}^1 & C_{23}^1 & 0 & 0 & 0 \\ C_{12}^1 & C_{23}^1 & C_{22}^1 & 0 & 0 & 0 \\ 0 & 0 & 0 & C_{44}^1 & 0 & 0 \\ 0 & 0 & 0 & 0 & C_{55}^1 & 0 \\ 0 & 0 & 0 & 0 & 0 & C_{55}^1 \end{pmatrix}, \quad C_{44}^1 = \frac{1}{2} (C_{22}^1 - C_{23}^1).$$

86

87 The following correction terms are given by Schön (2011, Table 6.15) for the case in  
 88 which the crack normals are aligned along the x-1 axis (x-axis), including the vertical  
 89 cracks:  
 90

91

$$C_{11}^1 = -\frac{(\lambda + 2\mu)^2}{\mu} \varepsilon U_3$$

92

$$C_{13}^1 = -\frac{\lambda (\lambda + 2\mu)^2}{\mu} \varepsilon U_3$$

93

$$C_{33}^1 = -\frac{\lambda^2}{\mu} \varepsilon U_3$$

94

$$C_{44}^1 = 0$$

95

$$C_{66}^1 = -\mu \varepsilon U_1$$

96

97 in which the correction terms  $C_{ij}^1$  are negative; thus, the elastic properties decrease with  
98 fracturing.  $U_1$  and  $U_3$  depend on the crack conditions (Mavko et al., 2009; Schon 2011).

99 For dry cracks,

100

$$U_1 = \frac{16(\lambda + 2\mu)}{3(3\lambda + 4\mu)}; \quad U_3 = \frac{4(\lambda + 2\mu)}{3(\lambda + \mu)}.$$

101

102 For wet cracks, Hudson's expressions for infinitely thin fluid-filled cracks are

103

$$U_1 = \frac{16(\lambda + 2\mu)}{3(3\lambda + 4\mu)}; \quad U_3 = 0.$$

104

105 Therefore, for the dry case,  $C_{ij}$  are

106

$$C_{11} = C_{11}^0 + C_{11}^1 = (\lambda + 2\mu)(1 - 6\varepsilon)$$

107

$$C_{13} = C_{13}^0 + C_{13}^1 = \lambda(1 - 6\varepsilon)$$

108

$$C_{33} = C_{33}^0 + C_{33}^1 = (\lambda + 2\mu)\left(1 - \frac{2}{3}\varepsilon\right)$$

109

$$C_{44} = C_{44}^0 + C_{44}^1 = \mu$$

110

$$C_{66} = C_{66}^0 + C_{66}^1 = \mu\left(1 - \frac{16}{7}\varepsilon\right).$$

112

113 For the wet case,

114

$$C_{11} = C_{11}^0 + C_{11}^1 = \lambda + 2\mu$$

115

$$C_{13} = C_{13}^0 + C_{13}^1 = \lambda$$

116

$$C_{33} = C_{33}^0 + C_{33}^1 = \lambda + 2\mu$$

117

$$C_{44} = C_{44}^0 + C_{44}^1 = \mu$$

118

$$C_{66} = C_{66}^0 + C_{66}^1 = \mu(1 - \frac{16}{7} \varepsilon) .$$

120

121  $C_{ij}$  has hexagonal symmetry with the x-1 axis (x-axis) expressed with five independent  
122 moduli.

123

124

125 **3.  $C'_{ij}(\varphi)$  elastic constants for rock material with vertical cracks that have an**  
126 **angle  $\varphi$  between the plane-normal direction and the x-1 axis (x-axis) (Figure**  
127 **S2c)**

128

129 When we rotate  $C_{ij}$  around the x-3 axis (z-axis) by an angle of  $\varphi$  from the x-1 axis (x  
130 axis),  $C_{ij}$  is a function of  $\varphi$ , as expressed by  $C'_{ij}(\varphi)$ .

131

132 Regarding coordinate transformations, the elastic compliances  $c_{ijkl}$  are, in general, fourth-  
133 rank tensors and hence transform according to

134

$$c'_{ijkl} = \beta_{ip}\beta_{jq}\beta_{kr}\beta_{ls}c_{pqrs},$$

136

137 where  $c'_{ijkl}$  and  $c_{pqrs}$  are the elastic compliances after and before the coordinate  
138 transformation, respectively. For rotation around the x-3 axis (z-axis),  $\beta_{ij}$  is the following  
139 matrix element

140

$$141 \begin{pmatrix} \cos\varphi & \sin\varphi & 0 \\ -\sin\varphi & \cos\varphi & 0 \\ 0 & 0 & 1 \end{pmatrix}.$$

142

143 In this study, we use the abbreviated 2-index Voigt notation  $C_{ij}$  instead of  $c'_{ijkl}$  and  $c_{ijkl}$ .  
144 Although an elastic constant looks like a second-rank tensor ( $C_{ij}$ ) with this notation, it is  
145 indeed a fourth-rank tensor; when one performs a coordinate transformation, one must go  
146 back to the full notation and follow the transformation rules for a fourth-rank tensor. The  
147 usual tensor transformation law is no longer valid. However, the change of coordinates  
148 for  $C_{ij}$  is more efficiently performed with the  $6 \times 6$  Bond Transformation Matrices,  $\mathbf{M}$   
149 (Mavko et al., 2009). The advantage of the Bond method for transforming compliances is  
150 that it can be applied directly to the elastic constants given in 2-index notation, as  
151 expressed as follows:

152

$$[C'] = [M][C][M]^T$$

153

154  $\mathbf{M}$

$$155 = \begin{bmatrix} \beta_{11}^2 & \beta_{12}^2 & \beta_{13}^2 & 2\beta_{12}\beta_{13} & 2\beta_{13}\beta_{11} & 2\beta_{11}\beta_{12} \\ \beta_{21}^2 & \beta_{22}^2 & \beta_{23}^2 & 2\beta_{22}\beta_{23} & 2\beta_{23}\beta_{21} & 2\beta_{21}\beta_{22} \\ \beta_{31}^2 & \beta_{32}^2 & \beta_{33}^2 & 2\beta_{32}\beta_{33} & 2\beta_{33}\beta_{31} & 2\beta_{31}\beta_{32} \\ \beta_{21}\beta_{31} & \beta_{22}\beta_{32} & \beta_{23}\beta_{33} & \beta_{22}\beta_{33} + \beta_{23}\beta_{32} & \beta_{21}\beta_{33} + \beta_{23}\beta_{31} & \beta_{22}\beta_{31} + \beta_{21}\beta_{32} \\ \beta_{31}\beta_{11} & \beta_{32}\beta_{12} & \beta_{33}\beta_{13} & \beta_{12}\beta_{33} + \beta_{13}\beta_{32} & \beta_{11}\beta_{33} + \beta_{13}\beta_{31} & \beta_{11}\beta_{32} + \beta_{12}\beta_{31} \\ \beta_{11}\beta_{21} & \beta_{12}\beta_{22} & \beta_{13}\beta_{23} & \beta_{22}\beta_{13} + \beta_{12}\beta_{23} & \beta_{11}\beta_{23} + \beta_{13}\beta_{21} & \beta_{22}\beta_{11} + \beta_{12}\beta_{21} \end{bmatrix}.$$

156

157 Then, we obtain  $C'_{ij}(\varphi)$  as

158

$$C'_{11}(\varphi) = \cos^4\varphi C_{11} + 2\sin^2\varphi \cos^2\varphi C_{12} + \sin^4\varphi C_{22} + 4\sin^2\varphi \cos^2\varphi C_{55}$$

159

$$C'_{22}(\varphi) = \sin^4\varphi C_{11} + 2\sin^2\varphi \cos^2\varphi C_{12} + \cos^4\varphi C_{22} + 4\sin^2\varphi \cos^2\varphi C_{55}$$

160

$$\begin{aligned} C'_{12}(\varphi) &= C'_{21}(\varphi) \\ &= \sin^2\varphi \cos^2\varphi C_{11} + (\sin^4\varphi + \cos^4\varphi) C_{12} + \sin^2\varphi \sin^2\varphi C_{22} \\ &\quad - 4\sin^2\varphi \cos^2\varphi C_{55} \end{aligned}$$

161

$$C'_{13}(\varphi) = C'_{31}(\varphi) = \cos^2\varphi C_{12} + \sin^2\varphi C_{23}$$

162

$$C'_{23}(\varphi) = C'_{32}(\varphi) = \sin^2\varphi C_{12} + \cos^2\varphi C_{23}$$

163

$$C'_{33}(\varphi) = C_{22}$$

164

$$C'_{44}(\varphi) = \cos^2\varphi C_{44} + \sin^2\varphi C_{55}$$

165

$$C'_{55}(\varphi) = \sin^2\varphi C_{44} + \cos^2\varphi C_{55}$$

166

$$167 C'_{66}(\varphi) = \sin^2\varphi \cos^2\varphi C_{11} - 2\sin^2\varphi \cos^2\varphi C_{12} + \sin^2\varphi \cos^2\varphi C_{22} + (\cos^2\varphi -$$

168

$$168 \sin^2\varphi)^2 C_{55}.$$

169

170 The following non-zero elements are zero in the next step 4, taking the rotational

171

$$173 C'_{16}(\varphi), C'_{61}(\varphi), C'_{26}(\varphi), C'_{62}(\varphi), C'_{36}(\varphi), C'_{63}(\varphi), C'_{45}(\varphi), C'_{54}(\varphi).$$

174

175

#### 176 **4. $\hat{C}_{ij}$ elastic constants for rock material with transversely isotropic symmetry**

177 **along the x-3 axis (z-axis) and a vertical crack distribution (Figure S2d)**

178

179 We took the rotational average of  $C_{ij}$  around the x-3 axis (z-axis) to obtain  $\hat{C}_{ij}$  that

180 showed transversely isotropic symmetry along the x-3 axis (z-axis) in the case of a

181 random vertical crack distribution as follows:

182

$$183 \hat{C}_{ij} = \frac{1}{2\pi} \int_0^{2\pi} C'_{ij}(\varphi) d\varphi,$$

184

185 which uses

186

$$\frac{1}{2\pi} \int_0^{2\pi} \sin^4 \varphi \, d\varphi = \frac{3}{8}, \quad \frac{1}{2\pi} \int_0^{2\pi} \cos^4 \varphi \, d\varphi = \frac{3}{8}, \quad \frac{1}{2\pi} \int_0^{2\pi} \sin^2 \varphi \cos^2 \varphi \, d\varphi = \frac{1}{8},$$

187

$$\frac{1}{2\pi} \int_0^{2\pi} \sin^2 \varphi \, d\varphi = \frac{1}{2}, \quad \frac{1}{2\pi} \int_0^{2\pi} \cos^2 \varphi \, d\varphi = \frac{1}{2}.$$

188

189  $\hat{C}_{ij}$  shows hexagonal symmetry or transversely isotropic symmetry with the x-3 axis (z-

190 axis) in which there are five independent constants:

191

$$\hat{C}_{11} = \frac{1}{2\pi} \int_0^{2\pi} C'_{11}(\varphi) \, d\varphi = \frac{3}{8} C_{11} + \frac{1}{4} C_{12} + \frac{3}{8} C_{22} + \frac{1}{2} C_{55}$$

192

$$\hat{C}_{12} = \frac{1}{2\pi} \int_0^{2\pi} C'_{12}(\varphi) \, d\varphi = \frac{1}{8} C_{11} + \frac{3}{4} C_{12} + \frac{1}{8} C_{22} - \frac{1}{2} C_{55}$$

193

$$\hat{C}_{13} = \frac{1}{2\pi} \int_0^{2\pi} C'_{13}(\varphi) \, d\varphi = \frac{1}{2} C_{12} + \frac{1}{2} C_{23}$$

194

$$\hat{C}_{33} = C_{22}$$

195

$$\hat{C}_{44} = \frac{1}{2\pi} \int_0^{2\pi} C'_{44}(\varphi) \, d\varphi = \frac{1}{2} C_{44} + \frac{1}{2} C_{55}$$

196

$$\hat{C}_{66} = \frac{1}{2\pi} \int_0^{2\pi} C'_{66}(\varphi) \, d\varphi = \frac{1}{8} C_{11} - \frac{1}{4} C_{12} + \frac{1}{8} C_{22} + \frac{1}{2} C_{55} = \frac{1}{2} (\hat{C}_{11} - \hat{C}_{12}).$$

197

198

199 **5. Wave velocities which propagate in the horizontal directions**

200

201 In the material with transversely isotropic symmetry, there are three modes of wave

202 propagation, and their velocities are dependent on the angle  $\theta$  between the axis of

203 symmetry (in this case, x-3 axis or z-axis) and the direction of the wave vector:

204

$$V_P = \sqrt{\frac{\hat{C}_{11} \sin^2 \theta + \hat{C}_{33} \cos^2 \theta + \hat{C}_{44} + A}{2\rho}}$$

205

$$V_{SV} = \sqrt{\frac{\hat{C}_{11} \sin^2 \theta + \hat{C}_{33} \cos^2 \theta + \hat{C}_{44} - A}{2\rho}}$$

206

$$V_{SH} = \sqrt{\frac{\hat{C}_{66} \sin^2 \theta + \hat{C}_{44} \cos^2 \theta}{2\rho}},$$

207

$$208 \text{ where } A = \sqrt{[(\hat{C}_{11} - \hat{C}_{44})\sin^2 \theta + (\hat{C}_{33} - \hat{C}_{44})\cos^2 \theta]^2 + (\hat{C}_{13} + \hat{C}_{44})^2 \sin^2 2\theta}.$$

209

210 For  $\theta = 90^\circ$ , the relationship simplifies to  $A = \hat{C}_{33} - \hat{C}_{44}$  and the wave velocity vectors  
 211 that propagate perpendicular to the x-3 axis in horizontal directions (Figure S1c) are

212

$$V_P = \sqrt{\frac{\hat{C}_{11}}{\rho}}, \quad V_{SV} = \sqrt{\frac{\hat{C}_{44}}{\rho}}, \quad V_{SH} = \sqrt{\frac{\hat{C}_{66}}{\rho}},$$

213

214 where  $V_P$ ,  $V_{SV}$ , and  $V_{SH}$  are the longitudinal-wave velocity, shear-wave velocity with  
 215 vertical polarization, and shear-wave velocity with horizontal polarization, respectively.

216

217 We consider low-porosity aggregate and flat cracks, and have ignored the effect of  
 218 porosity on the density of the composite (Anderson et al., 1974).

219 For the dry case, using  $\lambda = \mu$ ,

220

$$V_P^2 = \frac{\hat{C}_{11}}{\rho} = \frac{\lambda + 2\mu}{\rho} \left(1 - \frac{71}{21}\varepsilon\right) = V_{P0}^2 \left(1 - \frac{71}{21}\varepsilon\right)$$

221

$$V_{SV}^2 = \frac{\hat{C}_{44}}{\rho} = \frac{\mu}{\rho} \left(1 - \frac{8}{7}\varepsilon\right) = V_{SV0}^2 \left(1 - \frac{8}{7}\varepsilon\right)$$

222

$$V_{SH}^2 = \frac{\hat{C}_{66}}{\rho} = \frac{\mu}{\rho} \left(1 - \frac{15}{7}\varepsilon\right) = V_{SH0}^2 \left(1 - \frac{15}{7}\varepsilon\right),$$

223

224 where  $V$  with a subscript 0 are the velocities without cracks.

225

226 For the wet case,

227

$$V_P^2 = \frac{\hat{C}_{11}}{\rho} = \frac{\lambda + 2\mu}{\rho} \left(1 - \frac{8}{21}\varepsilon\right) = V_{P0}^2 \left(1 - \frac{8}{21}\varepsilon\right)$$

228

$$V_{SV}^2 = \frac{\hat{C}_{44}}{\rho} = \frac{\mu}{\rho} \left(1 - \frac{8}{7}\varepsilon\right) = V_{SV0}^2 \left(1 - \frac{8}{7}\varepsilon\right)$$

229

$$230 \quad V_{SH}^2 = \frac{\hat{C}_{66}}{\rho} = \frac{\mu}{\rho} \left(1 - \frac{8}{7}\varepsilon\right) = V_{SH0}^2 \left(1 - \frac{8}{7}\varepsilon\right).$$

231

232 The effect of cracks on velocity, in terms of the ratio of velocities with and without  
 233 cracks, is proportional to the crack density parameter  $\varepsilon$  at small values of  $\varepsilon$ :

234

$$\left(\frac{V}{V_0}\right)^2 = 1 - p_i \varepsilon .$$

235

236

237

238

239 **Figure S1.** The basic assumptions in this study: (a) the coordinate system, (b) vertical  
240 cross section of transversely isotropic rock with vertical cracks, and (c) side view of the  
241 direction of wave propagation and crack distribution.

242 **Figure S2.** Procedure for calculating the elastic constants in the transversely isotropic  
243 rock with vertical cracks: (a)  $\mathbf{C}_{ij}^0$  elastic constants of the rock matrix; (b)  $\mathbf{C}_{ij}$  elastic  
244 constants for the rock material with vertical cracks for which the plane-normal direction  
245 is along the x-1 axis (x-axis); (c)  $\mathbf{C}'_{ij}(\boldsymbol{\varphi})$  elastic constants for rock material with vertical  
246 cracks for which the angle between the plane-normal direction and the x-1 axis (x-axis) is  
247  $\boldsymbol{\varphi}$ ; and (d)  $\widehat{\mathbf{C}}_{ij}$  elastic constants for rock material with transversely isotropic symmetry  
248 along the x-3 axis (z-axis) with vertical cracks with random values of  $\boldsymbol{\varphi}$ .  
249